ROZPRAWY INŻYNIERSKIE • ENGINEERING TRANSACTIONS • 30, 2, 283—295, 1982
Polska Akademia Nauk • Instytut Podstawowych Problemów Techniki

THEORETICAL AND EXPERIMENTAL STUDIES OF THE DEVELOPING TURBULENT NON-NEWTONIAN FLOW IN A PIPE

M. H. EMBABY and A. VERBA (BUDAPEST)

A theoretical analysis is given for the developing turbulent non-Newtonian flow in a circular or a square cross section pipe. An experimental study on a square cross section pipe, using aqueous solutions of carboxymethyl cellulose as the non-Newtonian fluids, was carried out. Predictions of the pressure distribution and the critical Reynolds number are presented.

NOTATIONS

A n dependent constant,
a shape constant,
B n dependent constant,
b shape constant,
C shape factor,
C_f friction factor defined in Eq. (2.21),
D circular pipe diameter of square duct width,
H_1, H_2 total pressure tube calibration heads, (Fig. 3),
K incremental entrance pressure drop factor,
n flow behaviour index,
$P, \Delta p, \Delta p_e$ pressure, dimensionless pressure, dimensionless entrance pressure drop
r, R radial distance, pipe radius,
Re, Re Reynolds number defined in Eq. (2.4), distance Reynolds number $\dfrac{x^n U^{2-M}}{KC^n}$
$u, u^* = \sqrt{\dfrac{\tau_W}{d}}$ axial velocity, local shear velocity,
U_E, U_G, U_M velocities at the entrance, outside the boundary layer, mean, respectively
x, X_e axial coordinate, entrance length,
y, Y distance from pipe or duct wall, dimensionless hydraulic diameter
Z dimensionless boundary layer thickness,
δ boundary layer thickness,
η non-Newtonian consistency,
ξ dimensionless distance from the wall,
ρ mass density,
τ shear stress,
velocity superscript implies: velocity/u^*,
length superscript+ implies (length)^n $u^{*\,2-n}\rho/\eta$.

SUBSCRIPTS

c critical,
fd evaluated in the fully-developed flow,
l evaluated for laminar flow,

s evaluated at sections s-s (Figs. 1 and 2),
t evaluated for turbulent flow,
v evaluated at the viscous sublayer edge,
w evaluated at the pipe wall.

1. Introduction

Studies of the developing laminar Newtonian and non-Newtonian flows in a pipe have been carried out by many authors [1, 2 and 3]. Studies of turbulent Newtonian entrance zone flows have also been carried out [4 and 5]. Recently, such studies for drag reduction flows have appeared [6]. It has been noted that turbulent non-Newtonian (entrance zone) studies were confined to little experimental data [7, 8 and 9] while theoretical studies have not as yet appeared. The purpose of this work is to study theoretically and experimentally the turbulent non-Newtonian entrance zone flows in a circular or a square cross-section pipe.

2. Theoretical analysis

The present theoretical study follows and generalizes the previous procedure carried out with Newtonian [4] and drag reduction flows [6]. Thus it applies the momentum integral method and the continuity equation to the developing boundary layer in the pipe.

Momentum integral equation: Fig. 1 shows a model of a developing boundary layer in the entrance zone of a pipe. A force balance in the axial direction for an element of length dx of the boundary layer of thickness δ thus gives for a circular pipe

$$-\tau_w D dx - dp\delta(D-\delta) = 2d\left[\int_R^{R-\delta} \rho u^2 r dr\right] - 2U_G d\left[\int_R^{R-\delta} u r dr\right], \tag{2.1}$$

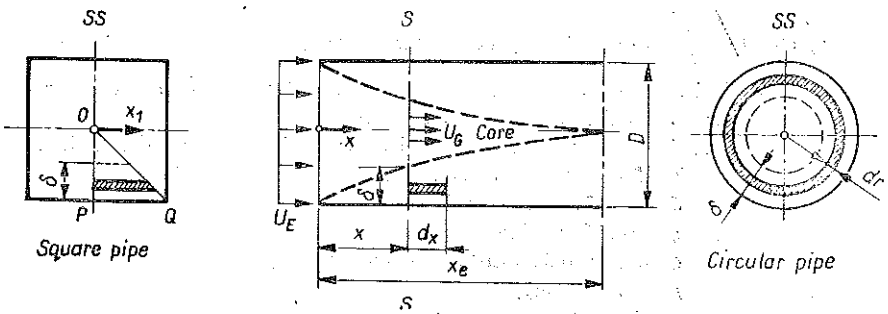

Fig. 1. Descriptive sketch of analysis symbols and coordinates used for a circular and a square cross-section pipe.

with $dP = -U_G\, dU_G$ in the core. Using the coordinate y (distance from the wall),

$$r = \frac{D}{2} - y,$$

Eq. (2.1) becomes

$$\frac{dx}{D}=\left(\frac{\rho}{\tau_w}\right)\frac{U_G}{D^2}\,\delta\,(D-\delta)\,dU_G-\left(\frac{\rho}{\tau_w}\right)\frac{2U_G}{D^2}\,d\left[-\int_0^{\delta}\left(u\frac{D}{2}-y\right)dy\right]- \tag{2.2}$$

$$-\left(\frac{\rho}{\tau_w}\right)\frac{2}{D^2}\,d\left[\int_0^{\delta}u^2\left(\frac{D}{2}-y\right)dy\right].$$

Continuity equation

Continuity requires the average velocity U_M to remain the same along the pipe, thus [4]

$$U_M D^2=8\int_0^{\delta}u\left(\frac{D}{2}-y\right)dy+U_G\,(D-2\delta)^2\,. \tag{2.3}$$

For a square pipe

Two basic assumptions are adapted in this case [4]: I. The Isolves are parallel to the duct walls. II. Corner effects, i.e. secondary flow effects, are neglected. Due to similarity only the triangle OPQ shown in the figure will be considered. A similar momentum balance and continuity equation application thus results in exactly the same mathematical equations (2.2) and (2.3), respectively. It must be noted that all the symbols have the same meaning with the exception of the symbol D which represents the duct width in this case.

General Reynolds number formula

In order to keep generality, a Reynolds number which includes the shape effect will be adapted [1] and it is given by

$$\mathrm{Re}=\frac{D_h^n\,U_M^{2-n}\,\rho}{8^{n-1}\,\eta c}, \tag{2.4}$$

where C is a factor including the shape effect and is given by

$$C=\left(\frac{a}{n}+b\right)^n, \tag{2.5}$$

where again a and b are shape constants given as:

$$\begin{aligned}&\text{for a circular pipe}\quad a=0.25,\quad b=0.75;\\ &\text{for a square pipe}\quad a=0.2121,\quad b=0.6766.\end{aligned} \tag{2.6}$$

It must be noted that Dh reduces to the pipe diameter for a circular pipe and to the duct width for a square one.

Velocity profiles in the developing boundary layer

For Power-law fluids, the fully-developed velocity profile, Fig. 2 line 013, has the form [8]

$$\begin{aligned}u^+&=(y^+)^{\frac{1}{n}}, \quad 0\leqslant y^+\leqslant y_v^+,\\ u^+&=A\ln y^+ +B, \quad y\leqslant y^+\leqslant R^+,\end{aligned} \tag{2.7}$$

where

$$u^+ = \frac{u}{u^*},$$

(2.8)

$$y^+ = y^n\, u^{*2-n}\frac{\rho}{\eta}$$

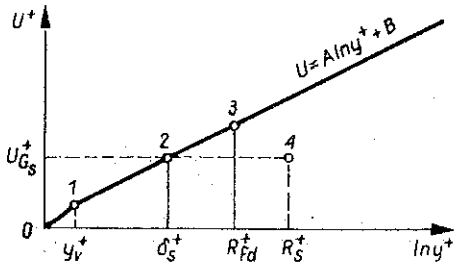

FIG. 2. Velocity profiles in the analysis.

and A, B are constants depending on the flow behaviour index n and given by

$$A = \frac{2.46}{(n)^{.75}},$$

(2.9)

$$B = \frac{3.475\left[1.96+0.81n-0.7n\,\ln\left(3+\frac{1}{n}\right)\right]}{(n)^{.75}} - \frac{0.566}{(n)^{1.2}}.$$

As to the developing boundary layer, the following assumptions will be used:

I. At the entrance the velocity distribution is uniform (Fig. 6).

$$u = U_E.$$

II. The turbulent boundary layer begins to develop at the entrance with thickness zero until full development with the thickness of a half-pipe diameter or duct width. Thus, at any section there is a turbulent boundary layer of thickness δ and a core of uniform velocity U_G, Fig. 1.

III. The distance from entrance X is considered to be implicitly included in the wall shear velocity $u^* = u^*(x)$. Thus, with dimensional analysis, [8], a profile similar to that given by Eqs. (2.7) will result. Neglecting the contributions by the viscous sublayer to the integrals in Eqs. (2.2) and (2.3), then at any section, section S-S in Fig. 1, the velocity profile will be that represented by line 1-2-4 in Fig. 2 and given by:

$$u^+ = A\ln y^+ + B, \qquad 0 \leqslant y^+ \leqslant +,$$

(2.10)

$$u^+ = u_G^+ = A\ln\delta^+ + B, \qquad \delta^+ \leqslant y^+ \leqslant R^+.$$

To make use of the above assumptions, the following dimensionless variables will be used:

Velocity

$$u^+ = \frac{u}{u^*}, \qquad U_M^+ = \frac{U_M}{u^*}.$$

(2.11)

Distance

$$y^+ = \frac{y^n u^{*2-n} \rho}{\eta},$$

$$\delta^+ = \frac{\delta^n u^{*2-n} \rho}{\eta}, \tag{2.12}$$

$$D^+ = \frac{D^n u^{*2-n} \rho}{\mu}.$$

Reynolds number

$$\mathrm{Re} = \frac{D^n U_M^{2-n} \rho}{\eta 8^{n-1} C}. \tag{2.13}$$

Integrating Eq. (2.2) from 0 to x and using the above dimensionless variables, rearranging gives

$$\frac{X}{D} = \int_1^{\frac{u_G^+}{u_M^+}} \left[U_G^+ \delta^{+\frac{1}{n}} (D^{+\frac{1}{n}} - \delta^{+\frac{1}{n}}) - 2 \int_0^{\delta^{+\frac{1}{n}}} u^+ \left(\frac{D^{+\frac{1}{n}}}{2} - y^{+\frac{1}{n}} \right) d\left(y^{+\frac{1}{n}} \right) \right] \times \tag{2.14}$$

$$\times \frac{U_M^+}{D^{+\frac{2}{n}}} d\left(\frac{U_G^+}{U_M^+} \right) + \int_a^b 2 U_M^{+2} d \left[\frac{1}{U_M^{+2} D^{+\frac{2}{n}}} \left\{ U_G^+ \int_0^{\delta^{+\frac{1}{n}}} u^+ \left(\frac{D^{+\frac{1}{n}}}{2} - y^{+\frac{1}{n}} \right) d \times \right. \right.$$

$$\left. \left. \times (y^{+\frac{1}{n}}) - \int_0^{\delta^{+\frac{1}{n}}} u^{+2} \left(\frac{D^{+\frac{1}{n}}}{2} - y^{+\frac{1}{n}} \right) d(y^{+\frac{1}{n}}) \right\} \right].$$

Similarly, Eq. (2.3) can be written as

$$(8^{n-1} C \, \mathrm{Re})^{\frac{1}{2-n}} D^{+\frac{4-3n}{n(2-n)}} = \tag{2.15}$$

$$= 8 \int_0^{\delta^{+\frac{1}{n}}} u^+ \left(\frac{D^{+\frac{1}{n}}}{2} - y^{+\frac{1}{n}} \right) d(y^{+\frac{1}{n}}) + U_G^+ (D^{+\frac{1}{n}} - 2\delta^{+\frac{1}{n}})^2.$$

Inspection of Eqs. (2.14) and (2.15) shows that the integrals appearing can easily be evaluated if the following variables are introduced:

$$\xi = y^{+\frac{1}{n}}, \qquad Z = \delta^{+\frac{1}{n}}, \qquad Y = D^{+\frac{1}{n}}. \tag{2.16}$$

Thus Eq. (2.14) reduces to

$$\frac{X}{D} = \int_i^{\frac{u_G^+}{u_M^+}} \left[U_G^+ Z (Y - Z) - 2 \int_0^Z u^+ \left(\frac{Y}{2} - \xi \right) d\xi \right] \frac{U_M^+}{Y^2} d\left(\frac{U_G^+}{U_M^+} \right) + \tag{2.17}$$

$$+ \int_a^b 2 U_M^{+2} d \left\{ \frac{1}{U_M^{+2} Y^2} \left[U_G^+ \int_0^Z u^+ \left(\frac{Y}{2} - \xi \right) d\xi - \int_0^Z u^{+2} \left(\frac{Y}{2} - \xi \right) \xi d \right] \right\}$$

and Eq. (2.15) to

$$(8^{n-1}\,C\,\mathrm{Re})^{\frac{1}{2-n}}\,Y^{\frac{4-3n}{2-n}}=8\int_0^Z u^+\left(\frac{Y}{2}-\xi\right)d\xi+U_G^+\,(Y-2Z)^2\,. \tag{2.18}$$

Rewriting the velocity profile, Eq. (2.10) in terms of the variables ξ and Z gives

$$\begin{aligned} &u^+=nA\ln\xi+B, \quad 0\leqslant\xi\leqslant Z;\\ &u^+=u_G^+=nA\ln Z+B, \quad Z\leqslant\xi\leqslant\frac{Y}{2}. \end{aligned} \tag{2.19}$$

Local coefficient of friction C_f

Defining C_f as

$$C_f=\frac{\tau_w}{0.5\rho U_M^2}=\frac{2}{U_M^{+2}}\,. \tag{2.20}$$

Using Eqs. $(2.12)_3$ and (2.13), this may be written as

$$C_f=2\cdot\frac{Y^{\frac{2n}{2-n}}}{\left[(C8^{n-1}\,\mathrm{Re})^{\frac{1}{2-n}}\right]^2}\,. \tag{2.21}$$

Pressure distribution Δp. In the core, the momentum balance gives

$$dP=-\rho U_G\,dU_G\,.$$

Normalizing with the average velocity U_M and integrating, we get

$$(\Delta\bar{p})_{\frac{D}{X}}=\frac{P_{E-p}}{0.5\rho\,U_M^2}=\left(\frac{U_G}{U_M}\right)^2-1\,. \tag{2.22}$$

Incremental entrance pressure drop factor K. It is defined as [6]: $K=\Delta p_e$ following the steps in reference [6]; it is then determined from

$$K=\left(\frac{U_G}{U_M}\right)_{fd}^2-1-4C_{f_{fd}}\left(\frac{Xe}{D}\right). \tag{2.23}$$

Procedure of calculations. For a certain power law fluid having a flow behaviour index n at a certain Reynolds number Re. At a boundary layer thickness Z of the developing boundary layer Eq. (2.18) gives the corresponding dimensionless diameter Y.

Then Eq. (2.21) gives the corresponding coefficient of friction C_f. Using Eqs. $(2.19)_2$, (2.20) and (2.22), the pressure drop is then obtained. The corresponding elements of the integrals of the dimensionless distance X/D, in Eq. (2.17), are then evaluated.

The above steps were repeated until full development was reached for different boundary layer thicknesses and numerical integration was used in order to determine the different distances from entrance.

Turbulence prediction

Basing on experimental stiudies, BOGUE [7] suggested a procedure for determining the critical Reynolds number Re for non-Newtonian pipe flows. As seen in Fig. (2.11), the plot $(\Delta\bar{p}_t/\Delta\bar{p}_L) - \mathrm{Re}\,(x)$ should give a critical distance Reynolds number $\mathrm{Re}\,(x)_c$. The critical Reynolds number Re_c is then determined from the following inequality:

$$\mathrm{Re}_c < \left[\frac{2\left(\mathrm{Re}\,(x)_c\right)^{\frac{1}{n}}}{\left(\frac{Xe}{\mathrm{R\,Re}}\right)_L} \right]^{\frac{n}{n+1}} . \tag{2.24}$$

The present theoretical predictions for turbulent flow were used with the available laminar flow data for a flow behaviour index $n=0.726$ in reference [7] and the results are shown in Figs. 10 and 11.

3. EXPERIMENTAL WORK

An experimental set-up (Fig. 3) was designed to study the flow characteristics in both the entrance and fully-developed zones in a square cross section pipe. The pipe was 2.5 cm wide and 370 cm long. An entrance section of a 15 cm diameter was fitted at the pipe entrance. A recirculation flow circuit was adapted as shown in Fig. 3.

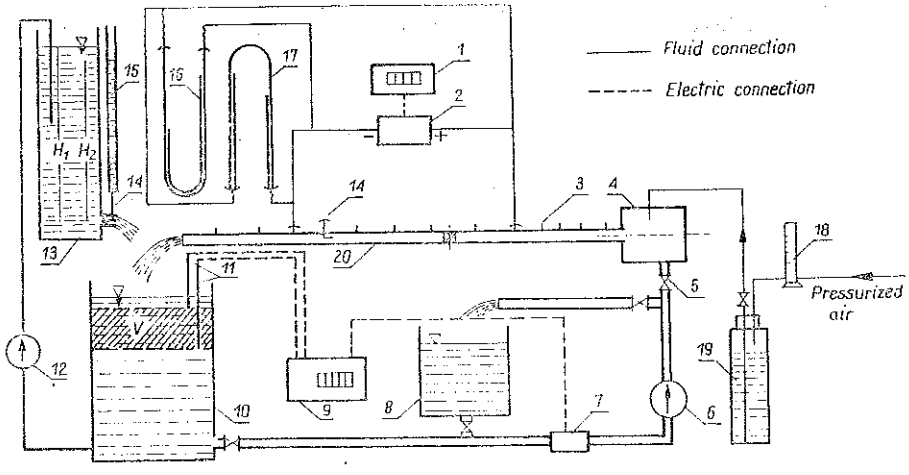

FIG. 3. Experimental setup. 1—digital multimeter, 2—pressure transducer, 3—pressure tap, 4—entrance chamber, 5—control valve, 6—circulating pump, 7—turbometer, 8—secondary tank, 9—pulse counter, 10—main circuit tank, 11—sensing conductors, 12—pump, 13—impact tube calibration tank, 14—impact tube, 15—piezometer tube, 16—mercury manometer, 17—water manometer, 18—rotameter, 19—concentrated polymer solution tank, 20—test pipe.

Solutions of carboxymethyl cellulose (CMC) were used as the non-Newtonian fluids for which the rheological parameters were determined using a rotary viscometer. A differential pressure transducer was used for pressure measurements while

a turbometer was used for flow rate measurements. Details of the measuring devices have been presented elsewhere [10].

4. Discussion

The expected theoretical effects of the Reynolds number Re and flow behaviour index n on the coefficient of friction C_f and pressure, Δp, distributions are shown in Fig. 4 to 7. The entrance zone pressure distribution has two characteristic pa-

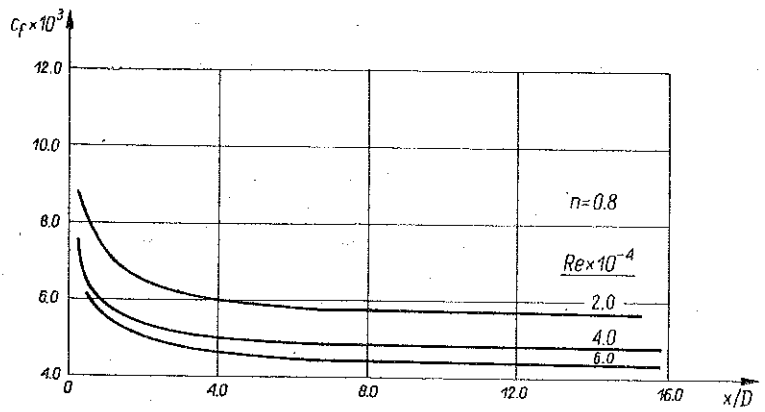

Fig. 4. Effect of Reynolds number Re on the coefficient of friction c_f.

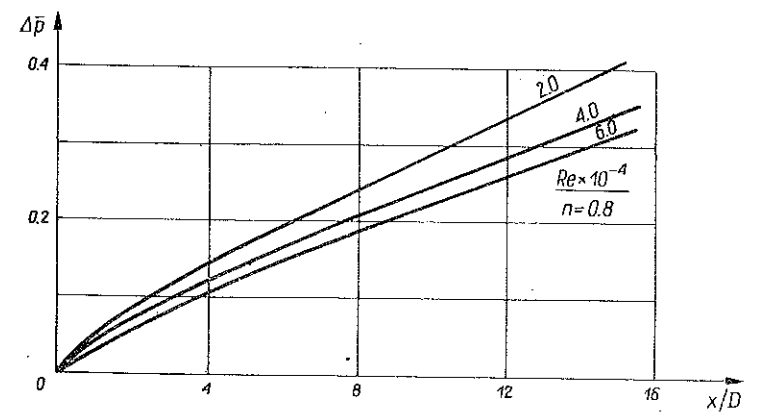

Fig. 5. Effect of Reynolds number e on the dimensionless pressure drop Δp.

rameters which are the entrance length X_e/L and the incremental entrance pressure drop K. Figures 8 and 9 show the behaviour of these parameters under the effect of Re and n. It must be noted that this discussion is restricted to square cross section predictions. Predictions of circular pipe have the same qualitative trends. Only for turbulence predictions, Figs. 10 and 11, are circular pipe predictions presented.

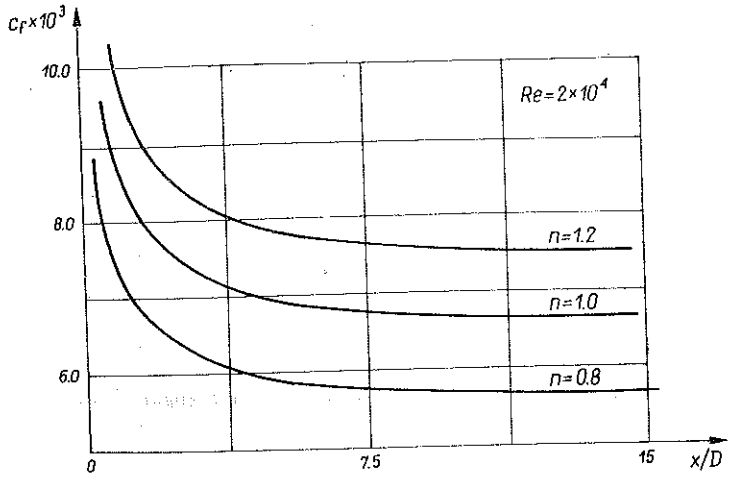

FIG. 6. Effect of flow behaviour index n on the coefficient of friction c_f.

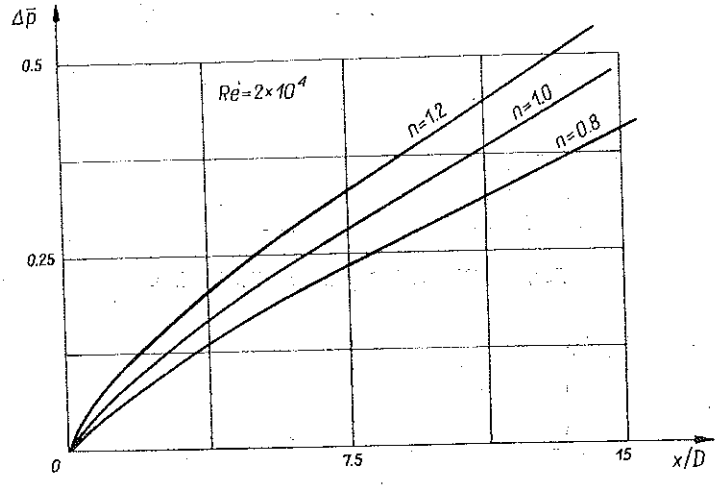

FIG. 7. Effect of flow behaviour index n on the dimensionless pressure drop Δp.

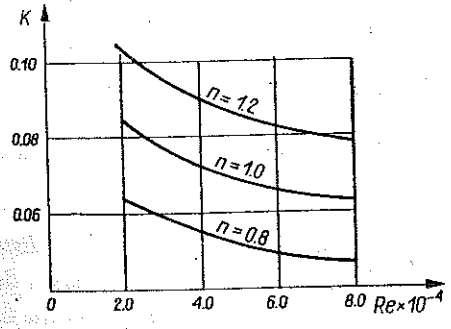

FIG. 8. Effect of Re and n on the incremental entrance pressure drop factor K.

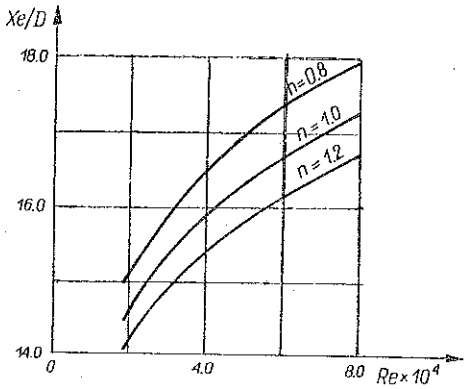

FIG. 9. Effect of Re and a on the entrance length Xe/D.

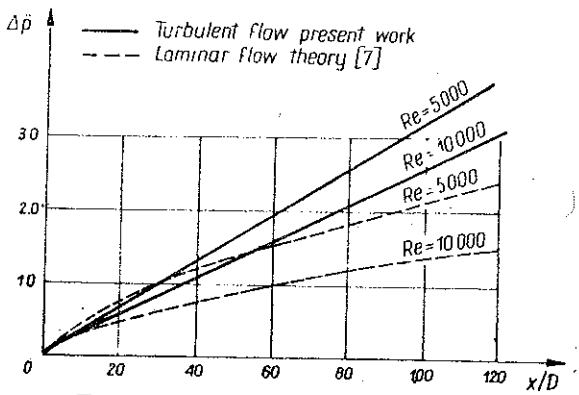

FIG. 10. Theoretical pressure distribution.

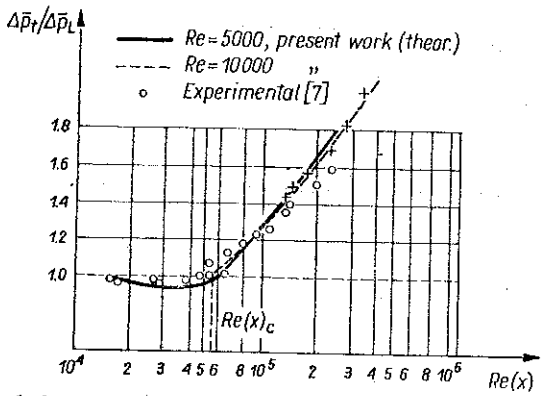

FIG. 11. Turbulent to laminar flow pressure against length Reynolds number.

The figures show the following:

I. Entrance zone coefficient of friction and pressure distributions

Effect of Re: for a certain n, the increase in Re has a decreasing effect on C_f, $\Delta\bar{p}$ and K as seen from Figs. 4, 5 and 8 respectively. On the other hand, the increase in Re has an increasing effect on X_e/D as shown in Fig. 9. Effect of n at a certain

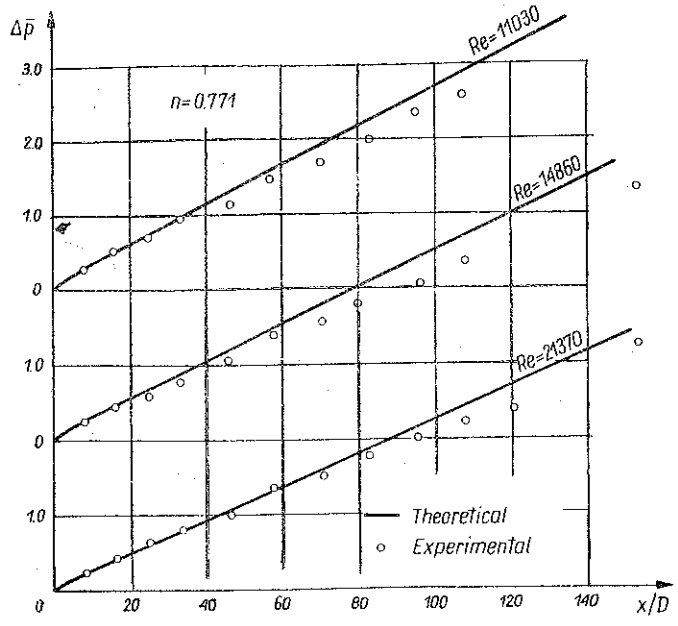

FIG. 12. Comparison between theoretical and experimental pressure distribution.

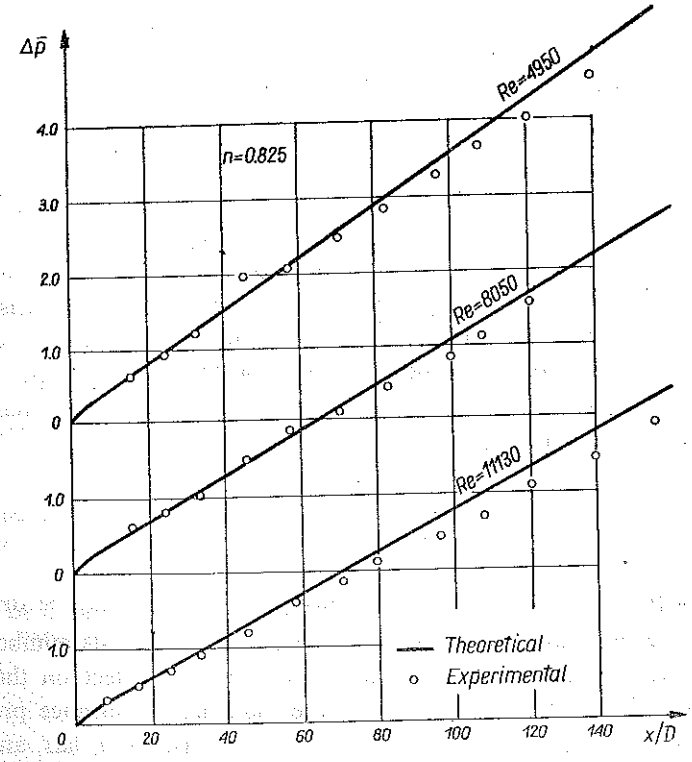

FIG. 13. Comparison between theoretical and experimental pressure distribution.

Re: the decrease in n has a similar effect on the flow parameters as that due to an increase in Re discussed above. Thus the decrease in n has a decreasing effect on C_f, $\Delta\bar{p}$ and K as shown in Fig. 6, 7 and 8 respectively. Also, the decrease in n has an increasing effect on X_e/D as shown in Fig. 9.

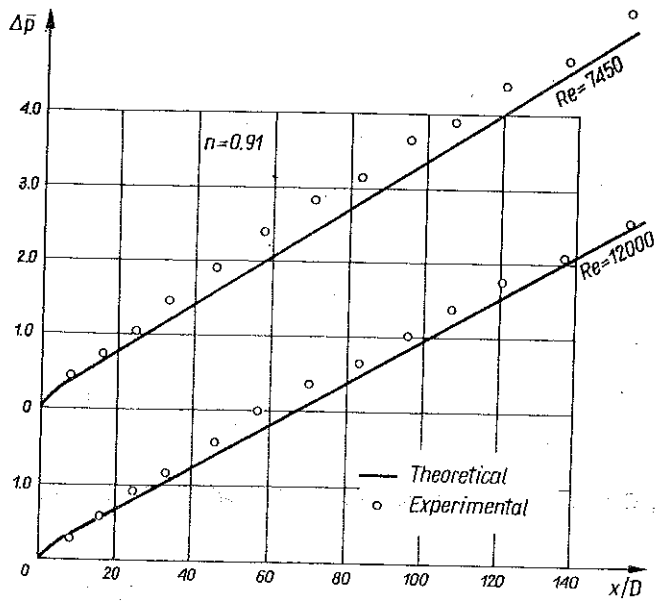

FIG. 14. Comparison between theoretical and experimental pressure distribution.

II. Turbulence prediction

Figure 11 shows the turbulence predicting plot for a flow behaviour index $n=0.726$. The resulting critical Reynolds number is $Re_c=2790$; this is an interesting result when compared to that given by Bogue as $Re_c=2600$. A series of measurements of the pressure distribution along the pipe are made and a comparison between theoretical and experimental findings are shown in Figs. 12 to 14. A reasonable quantitative agreement could be observed. Also Fig. 11 shows a comparison between the theoretical predictions based on the present work and those given by DODGE [7] where again a good agreement could be shown.

5. CONCLUSIONS

From the previous discussion the following conclusions may be drawn:

I. At any section along the pipe the increase in the Reynolds number Re or the decrease in the flow behaviour index n has a decreasing effect on the coefficient of friction C_f, the pressure drop $\Delta\bar{p}$ and the incremental entrance pressure drop K. On the other hand, the increase in Re or the decrease in n has an increasing effect on the entrance length X_e/D.

II. The present theoretical predictions could be used to determine the critical Reynolds number Re_c for pipe flows.

III. For design purposes entrance effects for non-Newtonian flows are not too different from those of Newtonian flows. The present predictions may be safely used either for circular or square cross section pipes.

References

1. H. W. Kozicki, C. H. Chou, and Tiu, Ch. Eng. Sci., **21**, 665, Feb. 1966.
2. R. A. Mashelkar, Proc. Instn. Mech. Engrs., **188**, 60/74, 683–89, 1975.
3. E. Salem and M. H. Embaby, Applied Scientific Res., **33**, 2, 119–39, 1977.
4. S. Ahmed and C. Brundrett, Int. J. Heat and Mass Transfer, 14, 365–75, 1971.
5. K. Knudsen and K. Katz, *Fluid dynamics and heat transfer*, Mc Graw Hill, 1958.
6. M. H. Embaby and A. Verba, Periodica Polytechnica, Chem. Eng., **24**, 1, 83–92, 1980.
7. D. C. Hogue, Ind. Engng. Chem., **51**, 874–78, 1959.
8. A. H. P. Skelland, *Non-Newtonian flow and heat transfer*, J. Willey, 1967.
9. D. W. Dodge and A. B. Metzner, AICHE J., **5**, 2, 189–204, 1959.
10. A. Verba, M. H. Embaby and I. Angyal, III, Aramlasmeresi Kollokvium in Miskolc, Hungary 1980.

Streszczenie

TEORETYCZNE I DOŚWIADCZALNE BADANIE ROZWOJU BURZLIWYCH PRZEPŁYWÓW NIENEWTONOWSKICH W RURZE

Przedstawiono analizę teoretyczną rozwoju burzliwego przepływu nienewtonowskiego w rurze o przekroju kołowym lub kwadratowym. Wykonano również badania eksperymentalne dla rury o przekroju kwadratowym stosując jako ciecz nienewtonowską roztwory wodne karboksy-metylocelulozy. Przedstawiono spodziewane rozkłady ciśnień i krytyczne liczby Reynoldsa.

Резюме

ТЕОРЕТИЧЕСКИЕ И ЭКСПЕРИМЕНТАЛЬНЫЕ ИССЛЕДОВАНИЯ РАЗВИТИЯ ТУРБУЛЕНТНЫХ НЕНЬЮТОНОВСКИХ ТЕЧЕНИЙ В ТРУБЕ

Представлен теоретический анализ развития турбулентного неньютоновского течения в трубе с круговым или квадратным сечениями. Проведены тоже экспериментальные исследования для трубы с квадратным сечением, применяя, как неньютоновскую жидкость, водные растворы карбоксиметилцеллюлозы. Представлены ожидаемые распределения давлений и критические числа Рейнольдса.

DEPARTMENT OF MECHANICAL ENGINEERING FOR THE CHEMICAL INDUSTRY
TECHNICAL UNIVERSITY, BUDAPEST, HUNGARY

Received October 22, 1981.